Chinese Journal of Catalysis 36 (2015) 1512–1518

available at www.sciencedirect.com

ScienceDirect

journal homepage: www.elsevier.com/locate/chnjc

Communication (Special Issue for Excellent Research Work in Recognition of Scientists Who Are in Catalysis Field in China)

Magnetic Co/Al_2O_3 catalyst derived from hydrotalcite for hydrogenation of levulinic acid to γ-valerolactone

Xiangdong Long, Peng Sun, Zelong Li, Rui Lang, Chungu Xia, Fuwei Li *

State Key Laboratory for Oxo Synthesis and Selective Oxidation, Lanzhou Institute of Chemical Physics, Chinese Academy of Sciences, Lanzhou 730000, Gansu, China

ARTICLE INFO

Article history:
Received 31 March 2015
Accepted 5 June 2015
Published 20 September 2015

Keywords:
Biomass conversion
Levulinic acid
γ-Valerolactone
Stable base metal catalyst
Core-shell structure
Cobalt

ABSTRACT

The efficient hydrogenation of levulinic acid (LA) to γ-valerolactone (GVL) over a hydrotalcite-derived non-precious metal Co/Al_2O_3 catalyst was achieved. Its core-shell structure and a strong interaction between Co and Al species stabilized the Co particles against leaching and sintering. This magnetic non-precious metal catalyst showed a comparable catalytic performance to a commercial Ru/C for the liquid hydrogenation of LA. It was easily separated from the reaction medium with an external magnet. The catalyst exhibited excellent recyclability, complete LA conversion and >99% GVL selectivity, and would be useful in a large scale biorefinery.

The hydrogenation of bio-derived levulinic acid (LA) and its esters [1–4] to γ-valerolactone (GVL) is a key reaction in sustainable biomass conversion because GVL can be widely used for fuel additive, food ingredient and as an intermediate for fine chemical production [5–8]. Both homogeneous and heterogeneous catalytic systems based on precious metal (Rh, Pd, Ir, Au, Ru) catalysts have been developed for efficient LA hydrogenation. Wright et al. [8] highlighted in their review that GVL production relied strongly on the use of noble metals, which could be an issue for the scale-up of the process due to their cost and the uncertain future availability. Although a few base metal heterogeneous catalysts have been successfully developed for this process [9–11], achieving a comparable activity and durability comparable with those of a low loading precious metal catalyst still remains a challenge due to their irreversible metal leaching and sintering, especially under liquid hydrogenation conditions [12].

We recently reported an ordered mesoporous carbon supported Ru-Ni bimetallic nanoparticle catalyst for the efficient conversion of LA into GVL [13]. We described here that a supported Co catalyst can be a suitable alternative for this interesting transformation. Co is widespread in the Earth, and Co-based catalysts have found wide application in the well-known Fisher-Tropsch synthesis [14,15] and other hydrogenation reactions [16,17]. Hydrotalcite-like compounds can be suitable precursors for the preparation of uniformly dispersed metal catalysts due to their tunable composition and confinement effect endowed by the interlayer galleries [18–22]. In the present work, we utilized an easily fabricated Co/Al-hydrotalcite (HT), a hydrated Co-Al hydroxide with a lamellar structure, as the single precursor to prepare an Al_2O_3 supported Co particle catalyst (Co/Al_2O_3), which possessed a

* Corresponding author. Tel/Fax: +86-931-4968528; E-mail: fuweili@licp.cas.cn
This work was supported by the National Natural Science Foundation of China (21133011, 21373246), Hundred-Talent Programme of the Chinese Academy of Sciences, and Lanzhou Institute of Chemical Physics, Chinese Academy of Sciences.
DOI: 10.1016/S1872-2067(15)60934-2 | http://www.sciencedirect.com/science/journal/18722067 | Chin. J. Catal., Vol. 36, No. 9, September 2015

relatively high surface area and strong interaction between the Co and Al species. The catalyst had a unique core-shell structure with amorphous alumina dominating the shell. These outstanding characteristics gave this Co/Al_2O_3 catalyst a comparable catalytic efficiency and recyclability with those of the representative noble metal catalyst Ru/C (LA conversion 80%; GVL selectivity 90%) in the conversion of LA to GVL [6].

In the present work, we used M/Al-HT (M = Co, Fe, Cu, Ni) as the precursor to prepare Al_2O_3 supported transition metal particles. The 4Co/Al-HT (n_{Co}/n_{Al} = 4) catalyst was prepared by a constant pH co-precipitation by following a reported procedure with a modification [23,24], which included the dropwise addition of an aqueous solution (100 mL) of Co (II) and Al (III) nitrates (total concentration of cations was 0.5 mol/L with a Co/Al ratio of 4 into 200 mL solution of Na_2CO_3 ($[Al^{3+}] = [CO_3^{2-}]$). The suspension pH was kept at 10.0 by the addition of NaOH aqueous solution (1.0 mol/L). The slurry was vigorously stirred at 80 °C during the solution addition. After the solution of metal cations was completely added, the suspension was stirred at 80 °C for 1 h, then followed by the step of precipitate aging at the same temperature for 18 h without stirring. The prepared hydrotalcite sample (denoted as 4Co/Al-HT) was reduced under H_2 (50 mL/min) at 700 °C for 2.5 h, affording the Co particle supported catalyst denoted as $4Co/Al_2O_3$. The other four catalysts ($5Co/Al_2O_3$, $3Co/Al_2O_3$, $2Co/Al_2O_3$, $1Co/Al_2O_3$) were prepared following the same procedure but with the molar ratios of Co/Al = 5, 3, 2 and 1. The Fe/Al_2O_3, Cu/Al_2O_3 and Ni/Al_2O_3 catalysts were synthesized following a similar procedure but using Fe (III), Cu (II) or Ni (II) nitrate as the precursor. The Co_3O_4 supported on the γ-Al_2O_3 precursor (Co/Al = 4) prepared by incipient wetness impregnation was denoted as Co_3O_4/γ-Al_2O_3, and the reduced catalyst $4Co/\gamma$-Al_2O_3 was prepared with the above reduction procedure. The 4Co/Al-HT hydrotalcite was first calcinated at 600 °C in air, then reduced under H_2 at 700 °C for 2.5 h. The sample was denoted as $4Co/Al_2O_3$-CR.

The conversion of levulinic acid to GVL was carried out in a 100 mL stainless steel autoclave equipped with a mechanical stirrer (Dalian Sanlin Instrument Co., China). A typical procedure was the following: LA 2.32 g (0.02 mol), catalyst Co/LA = 1.5% (molar ratio), solvent 30 mL, H_2 5 MPa, 180 °C, stirring rate 1000 r/min, 3 h. The liquid product was analyzed by a gas chromatograph (Agilent GC-7890A) equipped with a capillary column AT-SE-54 (60 m × 0.32 mm × 0.1 μm) and FID detector using diethylene glycol dimethyl ether as an internal standard. The qualitative identification of the products was achieved by GC-MS (Agilent 5975C/7890A).

Table 1
Catalytic performance of the base metal catalysts for the conversion of LA.

Entry	Catalyst	Conversion (%)	Selectivity (%)
1	$2Fe/Al_2O_3$	0.5	>99
2	$2Cu/Al_2O_3$	2	>99
3	$2Ni/Al_2O_3$	39	>99
4	$2Co/Al_2O_3$	43	>99
5	$1Co/Al_2O_3$	46	>99
6	$3Co/Al_2O_3$	43	>99
7	$4Co/Al_2O_3$	100	>99
8	$5Co/Al_2O_3$	93	>99
9	$4Co/\gamma$-Al_2O_3	29	>99
10	$4Co/Al_2O_3$-CR	69	>99
11	γ-Al_2O_3	—	—
12	Blank	—	—
13 [a]	$4Co/Al_2O_3$	6	>99
14 [b]	Ru/C	100	>99

Reaction conditions: LA 0.02 mol, catalyst Co/LA = 1.5% (molar ratio), 1,4-dioxane 30 mL, agitation rate 1000 r/min, H_2 5 MPa, 180 °C, 3 h. [a] Water used as solvent. [b] Ru/LA = 1.5% (molar ratio).

The results of the hydrogenation of LA to GVL over the HT-derived Co, Fe, Ni, Cu catalysts are summarized in Table 1. The $2Fe/Al_2O_3$ and $2Cu/Al_2O_3$ catalysts were almost inactive for LA hydrogenation. $2Ni/Al_2O_3$ showed moderate hydrogenation activity with 39% LA conversion. $2Co/Al_2O_3$ gave higher conversion (43%) of LA with >99% selectivity for GVL under the same reaction conditions, with no other hydrogenation product being detected in the product. Then we tested a series of HT-derived Co catalysts in which the Co/Al ratio was varied in the range of 1–5 (entries 5–8). The catalytic performance of the HT-derived Co catalyst was strongly dependent on the Co/Al ratio. The $4Co/Al_2O_3$ catalyst exhibited by far the highest catalytic activity (100% conversion) with a low catalyst loading (1.5% molar ratio of LA) and short time (3 h). Also, the selectivity to GVL remained >99%. Notably, the reference catalyst, Co supported on γ-Al_2O_3 prepared by impregnation with a Co/Al ratio of 4 only gave 29% of LA conversion (entry 9), suggesting that the catalyst preparation protocol greatly affected

Fuwei Li *got his Bachelor Degree in Chemical Engineering from Henan University in 2000, and received his Ph.D. degree in Physical Chemistry from Lanzhou Institute of Chemical Physics (LICP), Chinese Academy of Sciences (CAS) in 2005. He became a research assistant at the Institute of Process Engineering, Chinese Academy of Sciences in 2005, and then moved to the department of chemistry of the National University of Singapore in 2006 as a postdoctoral fellow. Since 2010, he is a full professor under "hundred talent" programme at LICP.* ***He has received*** *awards including* ***the Catalysis Rising Star Award*** *presented by The Catalysis Society of China* ***in 2012****. His research is devoted to catalyst design and investigations on their preparative chemistry to construct catalytic active centers for the activation of specific chemical bonds (such as C-H and C-O) and gas molecules (CO, H_2, O_2), to develop efficient and stable catalysts for the syntheses of valuable fine chemicals containing N and O atom. He has published more than 50 peer-reviewed papers with over 1300 citations (H factor is 22), 2 book chapters and 10 Chinese patents.*

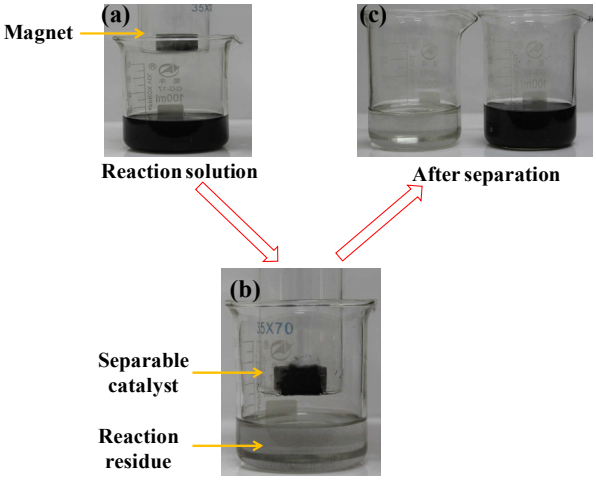

Fig. 1. Procedure for catalyst separation. (a) Mixture of catalyst and reaction solution; (b) magnetic catalyst was separated from the mixture by a magnet; (c) catalyst was suspended in water when the magnet was removed.

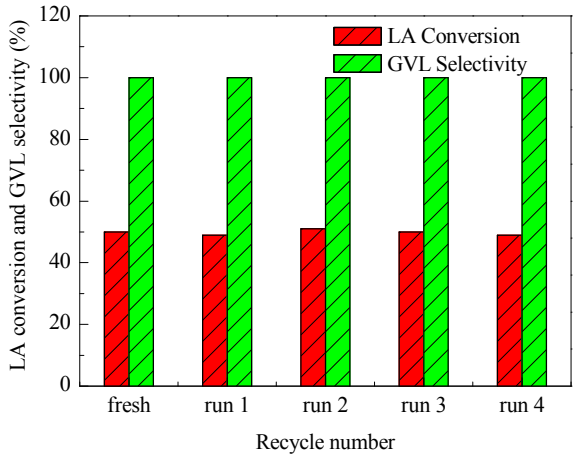

Fig. 2. Reusability of $4Co/Al_2O_3$ at 50% LA conversion. Reaction conditions: LA 0.06 mol, Co/LA = 0.4% (molar ratio), 1,4-dioxane 30 mL, agitation rate 1000 r/min, H_2 5 MPa, 180 °C, 3 h.

the catalytic performance. Furthermore, $4Co/Al_2O_3$-CR showed a lower LA conversion (69%) than $4Co/Al_2O_3$ in the hydrogenation reaction (entry 10), so we prepared the catalyst sample by directly reducing the hydrotalcite without the calcination step. The possible reason for this phenomenon is discussed below together with Fig. 7. GVL was not formed when pure γ-Al_2O_3 or no Co-catalyst was used in the reaction (entries 11 and 12), which confirmed that the presence of dispersed Co particles was essential for the high activity in the hydrogenation of LA. In particular, the conversion of LA dropped to 6% when water was used as the solvent (entry 13). The commercial Ru/C catalyst used in the hydrogenation of LA achieved excellent LA conversion and GVL selectivity (entry 14). By comparison, $4Co/Al_2O_3$ showed comparable catalytic performance with Ru/C in the liquid hydrogenative transformation to GVL.

One of the major issues for supported metal catalysts in the hydrogenation conversion of carboxylic acids in the liquid phase is their deactivation due to metal leaching and/or sintering, which are serious for the non-precious metal catalysts. Since carbonyl groups adsorb on metal nanoparticles, aggregation or even the formation of soluble metal-carbonyl complexes can occur especially when the interaction between the metal and support is not strong enough. To examine the stability of the optimal $4Co/Al_2O_3$ catalyst for GVL production, the reusability experiment of $4Co/Al_2O_3$ was carried out. To recycle the magnetic catalyst, a simple separation method was designed shown in Fig. 1, where a glass tube equipped with a permanent magnet was used. The spent $4Co/Al_2O_3$ was easily separated from the reaction mixture by the magnet. Since the surface of a Co nanoparticle was easily oxidized to cobalt oxide in air during the catalyst separation, before each run the separated catalyst was washed with distilled water and then reduced under H_2 flow (50 mL/min) at 700 °C for 1 h. After this treatment, the activity of the recovered catalyst was almost the same as in the first run (Fig. 2). The concentration of leached Co ion in the filtrate was measured as 8 ppm by ICP-AES, indicating that the Co/Al_2O_3 catalyst was stable enough in the liquid phase reaction and did not suffered severe deactivation under the relatively harsh conditions.

The HT-derived Co catalysts were characterized by N_2 adsorption isotherm, inductively coupled plasma atomic emission spectroscopy (ICP-AES), X-ray photoelectron spectroscopy (XPS), NH_3 temperature programmed desorption (NH_3-TPD), powder X-ray diffraction (XRD), H_2 temperature-programmed reduction (H_2-TPR), and transmission electron microscopy (TEM) to elucidate the origin of their high LA hydrogenation activity and stability. Typical data of the BET surface area, Co/Al ratio, acid amount, Co loading, and mean particle size are summarized in Table 2.

It can be seen that there was no apparent relationship between the BET surface area or total acid sites and the catalytic performance of the Co/Al_2O_3 samples, indicating the activity of the HT-derived samples was less associated with the external texture and acidity. However, associating the bulk and surface Co/Al ratio in Table 2 showed a good correlation between the

Table 2
Physicochemical properties of the Co/Al_2O_3 catalysts.

Sample	A_{BET} (m^2/g)	Bulk Co/Al [a] (molar ratio)	Surface Co/Al [b] (molar ratio)	Total acid sites [c] (mmol/g)	Co loading [d] (%)	Co particle size [e] (nm)
$1Co/Al_2O_3$	120.4	1.72	0.27	0.031	53.6	25.1
$2Co/Al_2O_3$	86.7	2.07	0.31	0.020	69.8	25.4
$3Co/Al_2O_3$	88.7	3.06	0.33	0.023	77.6	25.1
$4Co/Al_2O_3$	74.9	4.04	0.72	0.021	82.4	25.5
$5Co/Al_2O_3$	89.2	4.60	0.35	0.027	85.3	27.3

[a] Calculated by ICP-AES. [b] Determined from XPS. [c] Determined from NH_3-TPD. [d] Calculated by ICP-AES. [e] Calculated from TEM image.

Co content and the catalytic performance of the Co/Al_2O_3 catalysts. The surface Co/Al ratio of each sample was less than the corresponding bulk value, suggesting the catalyst surface was enriched in Al. The fact that the specific composition of the $4Co/Al_2O_3$ sample maximized the exposure of active Co species (highest surface Co/Al ratio) was crucial for achieving a high efficiency in the LA hydrogenation.

As for the five Co/Al-HT precursors, the XRD patterns showed the characteristic peaks of the hydrotalcite structure (Fig. 3) [25,26]. All samples have sharp diffraction peaks at 11.7°, 23.5°, 34.8°, 39.4°, 47.2°, 60.2°, 61.6°, which were indexed to the (003), (006), (009), (015), (018), (110), and (113) lattice planes of hydrotalcite, respectively. For the samples with the higher Co/Al molar ratio (5,4,3, and 2), only the hydrotalcite crystal phase was observed, suggesting the high purity of the hydrotalcite. However, there were both the hydrotalcite phase and Bayerite phase in the sample with the Co/Al molar ratio of 1, due to that the excess Al ions precipitated as an additional Bayerite phase [27,28].

After the reduction at 700 °C, the characteristic diffraction peaks of the hydrotalcite structure disappeared. Meanwhile, the major diffraction peaks with 2θ values of 44.3°, 51.6° and 76.1° (JCPDS 01-1255) ascribed to metal Co appeared (Fig. 4), indicating that the Co ions were reduced to metallic Co. During the catalyst screening, we found $4Co/Al_2O_3$ was the most efficient catalyst in the hydrogenation reaction of LA, so we looked for the explanation for its superior performance. When comparing the XRD patterns from these five Co/Al_2O_3 catalysts, obvious and wide diffraction peaks ascribed to the Co(100) and Co(101) planes were clearly observed in $4Co/Al_2O_3$. These results indicated that the Co(100) and Co(101) planes were highly active in the hydrogenation reaction, and the Co/Al_2O_3 catalyst exposed more of these two planes when the molar ratio of Co/Al = 4. We found that the used $4Co/Al_2O_3$ catalyst also maintained the Co and $CoAl_2O_4$ phases, which further confirmed the catalyst was stable under the reaction conditions.

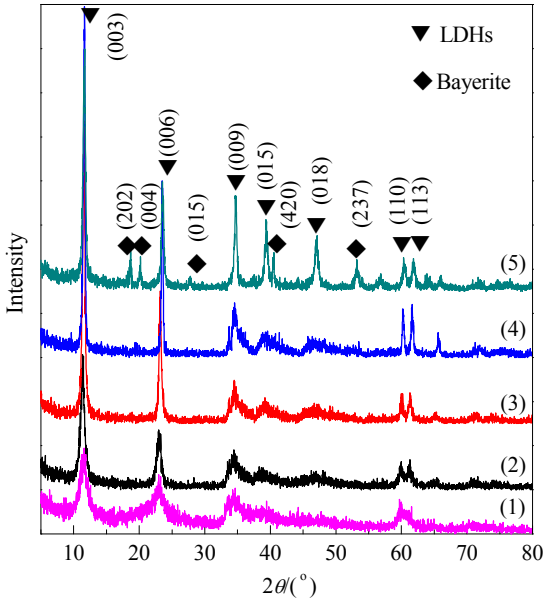

Fig. 3. XRD patterns of Co/Al-HT precursors. (1) 5Co/Al-HT; (2) 4Co/Al-HT; (3) 3Co/Al-HT; (4) 2Co/Al-HT; (5) 1Co/Al-HT.

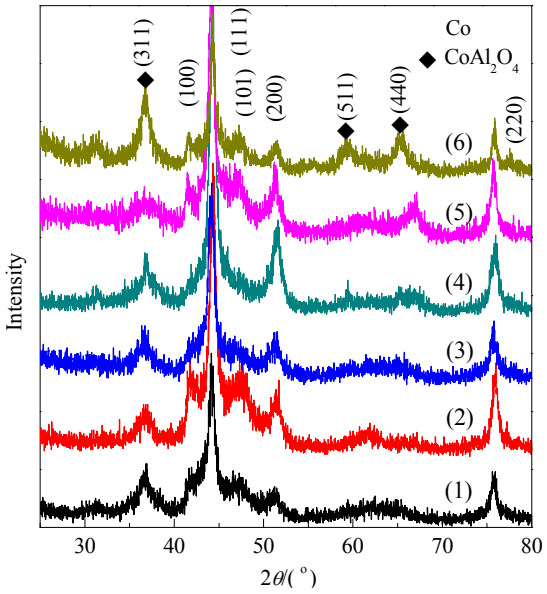

Fig. 4. XRD patterns of samples reduced with H_2. (1) $5Co/Al_2O_3$; (2) $4Co/Al_2O_3$; (3) $3Co/Al_2O_3$; (4) $2Co/Al_2O_3$; (5) $1Co/Al_2O_3$; (6) spent $4Co/Al_2O_3$.

The micro-structure and particle size distribution of the fresh and spent Co-based catalysts were characterized by TEM. As displayed in Fig. 5, the HT-derived Co catalysts showed the well dispersed nature of the Co nanoparticles. All of the fresh catalysts had particle sizes in the range of 25–30 nm (Table 2), indicating that the particle size of Co was not affected by its amount. However, the average Co particle size of $4Co/\gamma\text{-}Al_2O_3$ was larger than 200 nm (Fig. 5(5)). In view of the similar Co content in $4Co/\gamma\text{-}Al_2O_3$ and $4Co/Al_2O_3$, it was deduced that the

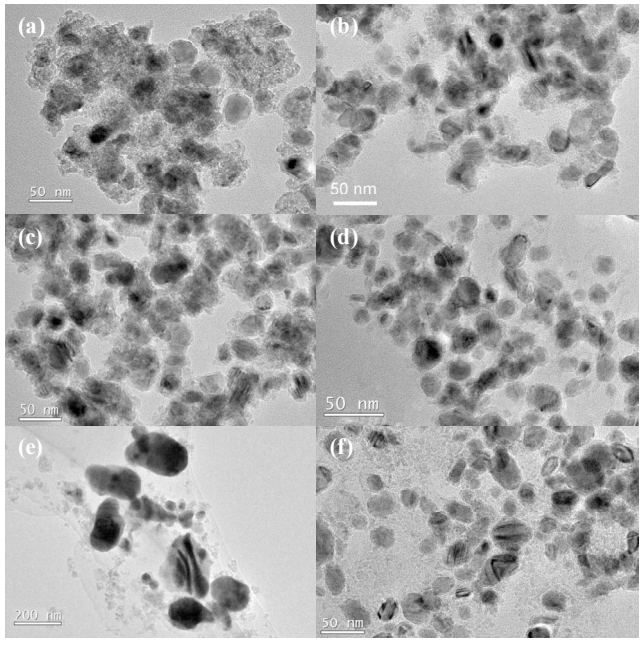

Fig. 5. TEM images of $1Co/Al_2O_3$-HT (a), $2Co/Al_2O_3$-HT (b), $3Co/Al_2O_3$-HT (c), $5Co/Al_2O_3$-HT (d), $4Co/\gamma\text{-}Al_2O_3$ (e), used $4Co/Al_2O_3$-HT (f).

difference in Co particle size was caused by the different preparation procedures. The remarkable difference in the microstructure between the $4Co/Al_2O_3$ and $4Co/\gamma\text{-}Al_2O_3$ catalysts manifested that the hydrotalcite was a good precursor for preparing well dispersed Co with a high loading. The TEM image of the used $4Co/Al_2O_3$ catalyst is shown in Fig. 5(6), and the mean particle size was calculated to be 25.6 nm, demonstrating no significant aggregation of Co particles occurred under the reaction conditions.

The structure of the most efficient $4Co/Al_2O_3$ catalyst was studied in detail to investigate its activity and stability (Fig. 6). It was clear that the Co particles have a core-shell structure (Figs. 6(a) and (b)). In the high resolution TEM (HRTEM) image, a dark core was surrounded by a light shell. The fast Fourier transform (FFT) patterns of the core are displayed in Fig. 6(d). It is common that the surface of the reduced Co nanoparticle is quickly oxidized to Co_3O_4 in air at room temperature. As for $4Co/Al_2O_3$, the surface composition also changed during the TEM sample preparation, and the corresponding FFT patterns are in good accordance with the Co_3O_4 (400), (222), and (331) planes (JCPDS 43-1003). In addition, no FFT dot was observed in the shell area, indicating that the shell was dominated by amorphous Al_2O_3. The composition of the Co/Al_2O_3 core-shell structure was further supported by that no impurity was observed in the energy dispersive X-ray (EDX) analysis (Fig. 6(f)). The above observations were consistent with the reported core-shell structure of $Co_4N\text{-}Al_2O_3$-HT, which also could be prepared with a high metal loading [29]. The surface Co/Al ratio of each sample (Table 2) was less than the corresponding bulk value, suggesting the catalyst surface was enriched in Al. Therefore, it was deduced that the particle core was composed of metal Co species while the shell was made up of amorphous Al_2O_3. This special core-shell structure prevented the sintering and leaching of the Co particles and resulted in the small particle sizes. In addition, compared with the fresh $4Co/Al_2O_3$, the XRD pattern (Fig. 4(f)) and TEM image (Fig. 5(f)) of the used catalyst did not show any obvious change. Therefore, both the core-shell structure and strong interaction of Co and Al species were responsible for the stability of the catalyst.

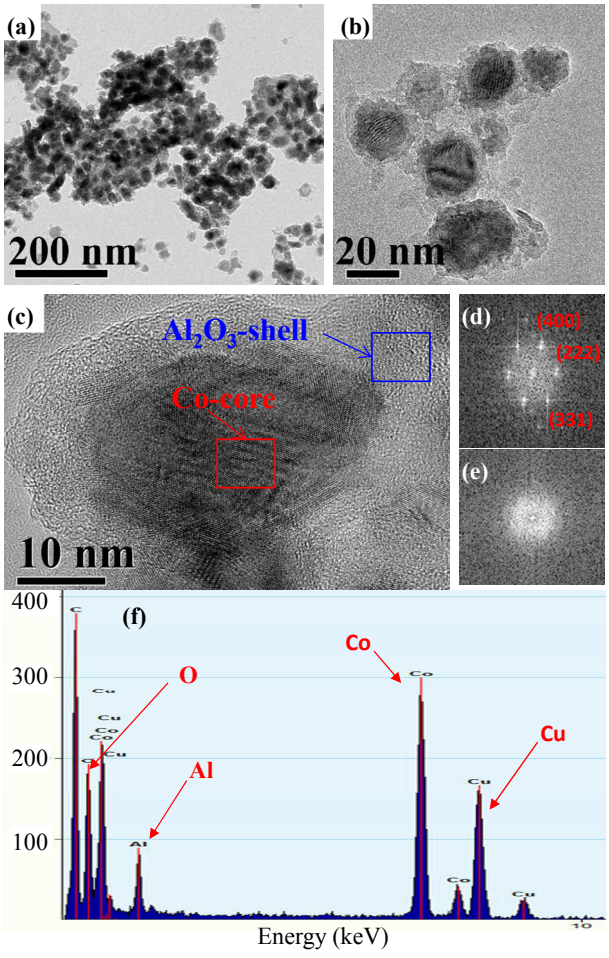

Fig. 6. TEM images of $4Co/Al_2O_3$. (a), (b) low magnification image, (c) HRTEM image, (d) FFT pattern of the red framed area in (c), (e) FFT pattern of the blue framed area in (c), (f) EDX image.

As discussed above with Table 1, entries 7 and 10, $4Co/Al_2O_3$-CR showed lower activity than $4Co/Al_2O_3$ in the hydrogenation of LA. TEM was used to compare their microstructure. The Co particle of $4Co/Al_2O_3$ was embedded in the Al shell and the average particle size was 25 nm (Fig. 7(a)). However, $4Co/Al_2O_3$-CR showed no core-shell structure, and the Co particle size was 54 nm (Fig. 7(b)). So we propose that the high activity for the reduced $4Co/Al_2O_3$ catalyst sample can be ascribed to its unique core-shell structure and small particle size.

To gain a deeper insight into the interaction between the supported phase and the carrier, H_2-TPR analysis was performed to observe the oxide reduction process. Figure 8 shows the H_2-TPR profiles of the $Co_3O_4/\gamma\text{-}Al_2O_3$ and Co/Al-HT catalyst precursors with different Co/Al ratios. Two sharp peaks (T_{max} = 220 and 311 °C) were observed with $Co_3O_4/\gamma\text{-}Al_2O_3$. Since Al_2O_3 cannot be reduced in this temperature range, the reduction peaks were due to the reduction of Co species. $Co_3O_4/\gamma\text{-}Al_2O_3$ was reduced in two steps at 220 and 311 °C yielding CoO and Co^0, respectively [30,31]. However, all the HT-derived samples showed one or two broad peaks from 500 to 700 °C. The T_{max} of the Co/Al-HT samples were located at 551, 605, 620, 631 and 647 °C for 5CoAl-HT, 4CoAl-HT, 3CoAl-HT, 2CoAl-HT, 1CoAl-HT, respectively. The shift to higher temperature revealed that the increase in Al amount in the samples hampered the reduction of Co ions [25]. In other words, there was a strong interaction between the Co ions and Al ions, which would prevent the sintering and leaching of Co nanoparticles.

The TPR results also reflected the strong interaction between Co and Al species in that the reduction temperature of $4Co/\gamma\text{-}Al_2O_3$ was below 350 °C, while those of the HT-derived Co catalysts were higher than 550 °C. From these observations,

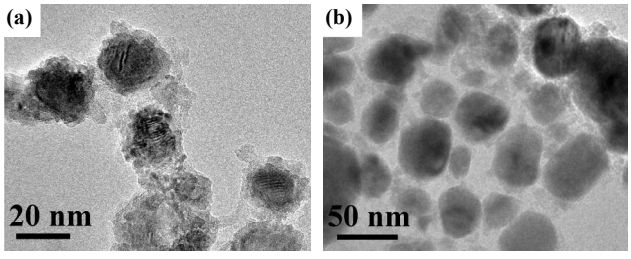

Fig. 7. TEM images of $4Co/Al_2O_3$ (a) and $4Co/Al_2O_3$-CR (b).

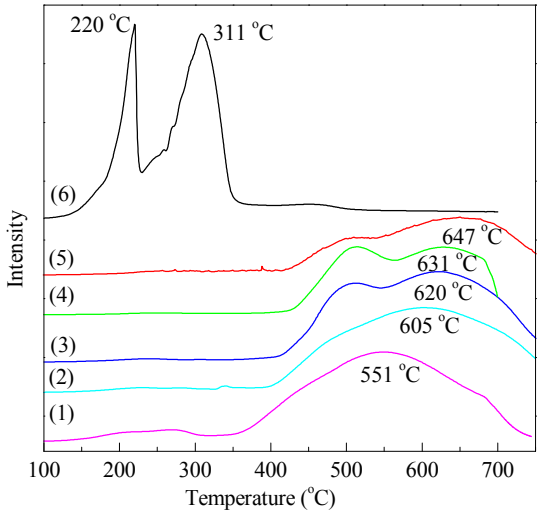

Fig. 8. H_2-TPR profiles of the Co/Al-HT precursors. (1) 5Co/Al-HT; (2) 4Co/Al-HT; (3) 3Co/Al-HT; (4) 2Co/Al-HT; (5) 1Co/Al-HT; (6) Co_3O_4/γ-Al_2O_3.

during the thermal treatment of the precursor under H_2 flow, the reduction of Co and the formation of the Co/Al core-shell structure simultaneously occurred. Consequently, the embedded Co nanoparticle is more difficult to reduce, so a broad TPR peak appeared at higher temperatures.

In summary, we developed an inexpensive and magnetic recyclable Co-based catalyst for the hydrogenation of LA to GVL. A unique core-shell Co/Al_2O_3 catalyst derived from hydrotalcite with a high Co loading was fabricated. The core-shell structure and strong interaction between Co and Al made the Co-based catalyst stable under the reaction conditions. These results also shed light on the rational design of efficient non-precious metal alternatives as heterogeneous catalysts.

References

[1] Tominaga K, Mori A, Fukushima Y, Shimada S, Sato K. *Green Chem*, 2011, 13: 810
[2] Lange J P, van de Graaf W D, Haan R J. *ChemSusChem*, 2009, 2: 437
[3] Gürbüz E I, Alonso D M, Bond J Q, Dumesic J A. *ChemSusChem*, 2011, 4: 357
[4] Alonso D M, Wettstein S G, Bond J Q, Root T W, Dumesic J A. *ChemSusChem*, 2011, 4: 1078
[5] Horvath I T, Mehdi H, Fabos V, Boda L, Mika L T. *Green Chem*, 2008, 10: 238
[6] Manzer L E. *Appl Catal A*, 2004, 272: 249
[7] Du X L, He L, Zhao S, Liu Y M, Cao Y, He H Y, Fan K N. *Angew Chem Int Ed*, 2011, 50: 7815
[8] Wright W R H, Palkovits R. *ChemSusChem*, 2012, 5: 1657
[9] Zhou H C, Song J L, Fan H L, Zhang B B, Yang Y Y, Hu J Y, Zhu Q G, Han B X. *Green Chem*, 2014, 16: 3870
[10] Hengne A M, Rode C V. *Green Che*m, 2012, 14: 1064
[11] Yuan J, Li S S, Yu L, Liu Y M, Cao Y, He H Y, Fan K N. *Energy Environ Sci*, 2013, 6: 3308
[12] Alonso D M, Wettstein S G, Dumesic J A. *Green Chem*, 2013, 15: 584
[13] Yang Y, Gao G, Zhang X, Li F W. *ACS Catal*, 2014, 4: 1419
[14] Bezemer G L, Bitter J H, Kuipers H P C E, Ooster-beek H, Holewijn J E, Xu X D, Kapteijn F, van Dillen A J, de Jong K P. *J Am Chem Soc*, 2006, 128: 3956
[15] Wang H, Zhou W, Liu J X, Si R, Sun G, Zhong M Q, Su H Y, Zhao H B, Rodriguez J A, Pennycook S J, Idrobo J C, Li W X, Kou Y, Ma D. *J Am Chem Soc*, 2013, 135: 4149
[16] Vigier K D O, Pouilloux Y, Barrault J. *Catal Today*, 2012, 195: 71
[17] Lee J, Jackson D H K, Li T, Winans R E, Dumesic J A, Kuechab T F, Huber G W. *Energy Environ Sci*, 2014, 7: 1657
[18] He L, Huang Y Q, Wang A Q, Wang X D, Chen X W, Delgado J J, Zhang T. *Angew Chem Int Ed*, 2012, 51: 6191
[19] Zhao M Q, Zhang Q, Zhang W, Huang J Q, Zhang Y H, Su D S, Wei F. *J Am Chem Soc*, 2010, 132: 14739
[20] An Z, He J, Duan X. *Chin J Catal*, 2013, 34: 225
[21] He J, Shi H M, Shu X, Li M L. *AIChE J*, 2010, 56: 1352
[22] Wu G W, Zhang C X, Li S R, Huang Z Q, Yan S L, Wang S P, Ma X B, Gong J L. *Energy Environ Sci*, 2012, 5: 8942
[23] Tsyganok A I, Tsunoda T, Hamakawa S, Suzuki K, Takehira K, Hayakawa T. *J Catal*, 2003, 213: 191
[24] Bai Z M, Wang Z Y, Zhang T G, Fu F, Yang N. *Appl Clay Sci*, 2012, 59: 36
[25] Gabrovska M, Edreva-Kardjieva R, Tenchev K, Tzvetkov P, Spojakina A, Petrov L. *Appl Catal A*, 2011, 399: 242
[26] Xia S X, Nie R F, Lu X Y, Wang L N, Chen P, Hou Z Y. *J Catal*, 2012,

Graphical Abstract

Chin. J. Catal., 2015, 36: 1512–1518 doi: 10.1016/S1872-2067(15)60934-2

Magnetic Co/Al_2O_3 catalyst derived from hydrotalcite for hydrogenation of levulinic acid to γ-valerolactone

Xiangdong Long, Peng Sun, Zelong Li, Rui Lang, Chungu Xia, Fuwei Li *
Lanzhou Institute of Chemical Physics, Chinese Academy of Science

A non-precious metal Co/Al_2O_3 catalyst prepared by reduction of a hydrotalcite precursor hydrogenated levulinic acid to γ-valerolactone with high efficiency and stability.

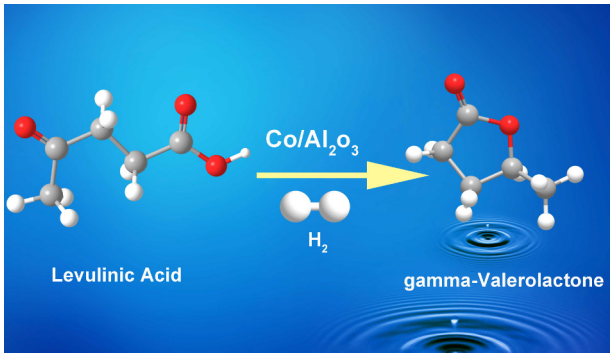

296: 1
[27] Perrotta A J, Tzeng S Y, Imbrogno W D, Rolles R, Weather M S. *J Mater Res*, 1992, 7: 3306
[28] Britto S, Kamath P V. *Inorg Chem*, 2010, 49: 11370
[29] Cheng H K, Huang Y Q, Wang A Q, Wang X D, Zhang T. *Top Catal*, 2009, 52: 1535
[30] Khassin A A, Yurieva T M, Kustova G N, Itenberg I S, Demeshkina M P, Krieger T A, Plyasova L M, Chermashentseva G K, Parmon V N. *J Mol Catal A*, 2001, 168: 193
[31] Arnoldy P, Moulijn J A. *J Catal*, 1985, 93: 38